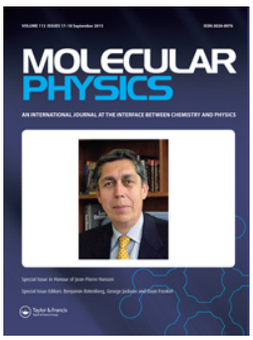

Taylor & Francis
Taylor & Francis Group

Molecular Physics

An International Journal at the Interface Between Chemistry and Physics

ISSN: 0026-8976 (Print) 1362-3028 (Online) Journal homepage: http://www.tandfonline.com/loi/tmph20

Deterministic time-reversible thermostats: chaos, ergodicity, and the zeroth law of thermodynamics

Puneet Kumar Patra, Julien Clinton Sprott, William Graham Hoover & Carol Griswold Hoover

To cite this article: Puneet Kumar Patra, Julien Clinton Sprott, William Graham Hoover & Carol Griswold Hoover (2015) Deterministic time-reversible thermostats: chaos, ergodicity, and the zeroth law of thermodynamics, Molecular Physics, 113:17-18, 2863-2872, DOI: 10.1080/00268976.2015.1026856

To link to this article: http://dx.doi.org/10.1080/00268976.2015.1026856

Published online: 31 Mar 2015.

Molecular Physics, 2015
Vol. 113, Nos. 17–18, 2863–2872, http://dx.doi.org/10.1080/00268976.2015.1026856

INVITED ARTICLE

Deterministic time-reversible thermostats: chaos, ergodicity, and the zeroth law of thermodynamics

Puneet Kumar Patra[a,*], Julien Clinton Sprott[b], William Graham Hoover[c] and Carol Griswold Hoover[c]

[a]*Advanced Technology Development Center, Indian Institute of Technology Kharagpur, Kharagpur, India;* [b]*Department of Physics, University of Wisconsin-Madison, Madison, WI, USA;* [c]*Ruby Valley Research Institute, Ruby Valley, NV, USA*

(*Received 21 January 2015; accepted 3 March 2015*)

The relative stability and ergodicity of deterministic time-reversible thermostats, both singly and in coupled *pairs*, are assessed through their Lyapunov spectra. Five types of thermostat are coupled to one another through a single Hooke's-law harmonic spring. The resulting dynamics shows that three specific thermostat types, Hoover–Holian, Ju–Bulgac, and Martyna–Klein–Tuckerman, have very similar Lyapunov spectra in their equilibrium four-dimensional phase spaces and when coupled in equilibrium or nonequilibrium pairs. All three of these oscillator-based thermostats are shown to be *ergodic*, with smooth analytic Gaussian distributions in their extended phase spaces (coordinate, momentum, and two control variables). Evidently these three ergodic and time-reversible thermostat types are particularly useful as statistical-mechanical thermometers and thermostats. Each of them generates Gibbs' universal canonical distribution internally as well as for systems to which they are coupled. Thus they obey the zeroth law of thermodynamics, as a good heat bath should. They also provide dissipative heat flow with relatively small nonlinearity when two or more such temperature baths interact and provide useful deterministic replacements for the stochastic Langevin equation.

Keywords: chaotic dynamics; time reversibility; temperature; thermostats; chaos; zeroth law

1. Deterministic time-reversible thermostats and ergodicity

In the early days of equilibrium many-body simulation, intercomparisons of results from constant-temperature Monte Carlo with those from constant-energy molecular dynamics were indirect, requiring the conversion of isothermal *NVT* data to isoenergetic *NVE* data. Only for hard disks and hard spheres, where temperature and energy are proportional, are the two ensembles identical [1].

Shuichi Nosé provided a conceptual breakthrough linking temperature T and energy E by discovering an isothermal canonical-ensemble molecular dynamics [2,3]. He started out by including an additional time-reversible 'time-scaling variable' s in his novel Hamiltonian:

$$\mathcal{H}_{\text{Nosé}} \equiv [K(p)/s^2] + \Phi(q) + (p_s^2/2M) + (\#kT/2)\ln(s^2). \quad (1)$$

Here # is the number of degrees of freedom, *including* s, and p_s is the momentum conjugate to s. M is a free parameter. Getting to the canonical ensemble from Nosé's Hamiltonian equations of motion requires just two more steps; (1) 'scaling the time', multiplying all of Nosé's time derivatives by s:

$$\{\dot{q} \to s\dot{q}\ ;\ \dot{p} \to s\dot{p}\};\ \dot{s} \to s\dot{s};\ \dot{p}_s \to s\dot{p}_s; \quad (2)$$

then (2) replacing all the scaled momenta $\{(p/s)\}$ by $\{p\}$. Nosé showed that the resulting distribution for the $\{q, p\}$ is Gibbs' canonical distribution.

Starting instead with the 'Nosé–Hoover' equations of motion [4–7],

$$\{\dot{q} = (p/m);\ \dot{p} = F(q) - \zeta p\};\quad \dot{\zeta} = \sum^{\#=ND} [(p^2/mkT) - 1]/\tau^2. \quad (3)$$

Hoover showed that Gibbs' canonical distribution, with s absent and with $\# = ND$ *not* including that extraneous s variable, is a stationary solution of the extended phase-space continuity equation,

$$(\partial f/\partial t) = 0 = -\sum^{\#}(\partial f\dot{q}/\partial q) - \sum^{\#}(\partial f\dot{p}/\partial p) - (\partial f\dot{\zeta}/\partial\zeta). \quad (4)$$

* Corresponding author Email: puneetpatra@atdc.iitkgp.ernet.in

Here ζ is a 'friction coefficient' proportional to Nosé's p_s and the free parameter τ takes the place of Nosé's parameter M. The stationary distribution function for the Nosé–Hoover motion equations is canonical in $\{q, p\}$ and Gaussian in the friction coefficient ζ:

$$f(q, p, \zeta) \propto e^{-\mathcal{H}/kT} e^{-\tau^2\zeta^2/2};\ \mathcal{H} = \Phi(q) + K(p). \quad (5)$$

The relaxation time τ controls the decay rate of velocity fluctuations in a D-dimensional N-body Hamiltonian system.

In order for averages using the Nosé–Hoover equations to agree with canonical-ensemble averages, it is necessary in principle that the dynamics be 'ergodic', meaning that it must reach all of the $\{q, p\}$ phase-space states. Of course in practice only a representative sampling of such states can be achieved. Whether or not the motion equations are 'ergodic' in this sense, *capable* of reaching all of the states described by Gibbs' canonical ensemble, depends upon the details of the underlying Hamiltonian $\mathcal{H}(q, p)$. For a single harmonic oscillator Hoover pointed out [5] that neither the four original unscaled Nosé equations nor the three Nosé–Hoover motion equations are ergodic:

$$\begin{aligned} \dot{q} &= +(p/s^2);\ \ \dot{p} = -q; \\ M\ddot{s} &= \dot{p}_s = [(p^2/s^3) - (2/s)];\ \text{(Nosé, not ergodic).} \\ \dot{q} &= +p;\ \dot{p} = -q - \zeta p; \\ \dot{\zeta} &= [p^2 - 1]/\tau^2;\ \text{(Nosé–Hoover, not ergodic).} \end{aligned} \quad (6)$$

These Nosé equations are singular while the Nosé–Hoover equations are not.

With the relaxation time τ equal to unity, numerical Nosé–Hoover calculations show that about 6% of the initial conditions drawn from the Gaussian distribution $e^{-q^2/2}e^{-p^2/2}e^{-\zeta^2/2}$ are chaotic, making up a 'chaotic sea' in the (q, p, ζ) space which is penetrated by an infinite number of holes. The remaining 94% of initial conditions generate regular periodic toroidal solutions which fill in these holes. Evidently this Nosé–Hoover thermostatted oscillator is far from 'ergodic' (where in this case an ergodic solution would have a smooth analytic Gaussian density throughout (q, p, ζ) space):

$$f_{\text{Gibbs}}(q, p, \zeta) \propto e^{(-q^2/2)}e^{(-p^2/2)}e^{(-\zeta^2/2)}\ \text{(ergodic).} \quad (7)$$

In 1990 Bulgac and Kusnezov reiterated the usefulness of the phase-space continuity equation in formulating more complicated motion equations (with two or three thermostatting control variables). Shortly thereafter they were able to use this approach to fill out the complete Gibbs' distribution for prototypical Hamiltonian systems like the harmonic oscillator and the two-well 'Mexican hat' problems [8–10].

There is no *foolproof* test for ergodicity. The only reliable diagnostic for space-filling ergodicity is the Lyapunov spectrum [11–19]. If this spectrum, which measures the long-time-averaged sensitivity of the dynamics to initial conditions, is not only chaotic, but also the *same* for *all* initial conditions, the system is likely ergodic. For the harmonic oscillator this means that *all* (q, p) oscillator states, all the way to infinity, will *eventually* occur. In nonergodic systems the long-time-averaged spectrum depends upon the initial conditions. In ergodic systems the long-time spectrum is always the same. By 1996 there were three known simple types of differential equations (HH = Hoover–Holian, JB = Ju–Bulgac, MKT = Martyna–Klein–Tuckermann) which were thought to produce ergodicity in a one-dimensional harmonic oscillator [9,17–19]. In addition to propagating the phase variables (q, p) all three included *two* additional control variables (ζ, ξ) capable of generating Gibbs' canonical distribution. For the simple harmonic oscillator these three models take the form

$$\begin{aligned} \{\dot{q} &= p;\ \dot{p} = -q - \zeta p - \xi p^3; \\ \dot{\zeta} &= p^2 - T;\ \dot{\xi} = p^4 - 3Tp^2\}\ \text{(HH);} \end{aligned}$$

$$\begin{aligned} \{\dot{q} &= p;\ \dot{p} = -q - \zeta^3 p - \xi p^3; \\ \dot{\zeta} &= p^2 - T;\ \dot{\xi} = p^4 - 3Tp^2\}\ \text{(JB) ;} \end{aligned}$$

$$\begin{aligned} \{\dot{q} &= p;\ \dot{p} = -q - \zeta p; \\ \dot{\zeta} &= p^2 - T - \xi\zeta;\ \dot{\xi} = \zeta^2 - T\}\ \text{(MKT).} \end{aligned}$$

So far no one-thermostat oscillator system (with just a single control variable) has been shown to be ergodic though it certainly is possible that such a one will be discovered. We explicitly include the temperature T in all of these models in order to set the stage for *nonequilibrium* systems incorporating both 'cold' and 'hot' degrees of freedom. It is worth pointing out that not all two-thermostat oscillator systems are ergodic. Patra and Bhattacharya showed that their very reasonable set of doubly thermostatted oscillator equations is not ergodic [14,19] :

$$\begin{aligned} \{\dot{q} &= p - \xi q;\ \dot{p} = -q - \zeta p;\ \dot{\zeta} = p^2 - T; \\ \dot{\xi} &= q^2 - T\}\text{(PB).} \end{aligned} \quad (8)$$

Our work here has three different aspects. First we explore the equilibrium Lyapunov instability which facilitates the ergodicity of all three (HH, JB, and MKT) thermostats. In the equilibrium case, where the phase-space distribution is a smooth Gaussian, the Lyapunov instability embedded in that Gaussian has a totally different multifractal character. We show that in equilibrium HH, JB, and MKT thermostats obey the zeroth law when coupled with one another or with other Hamiltonian systems. These thermostats can therefore produce Gibbs' complete canonical distribution provided that any internal energy barrier is not too large relative to kT. Second we consider *nonequilibrium* cases,

where heat flows between thermostats with the thermostat temperatures set at different values. The nonequilibrium dynamics is still ergodic but the phase-space distribution is no longer a smooth Gaussian. It is instead an intimate multifractal combination of the attractor–repellor pairs common to macroscopic time-reversible, but dissipative, systems. We also illustrate the application of ergodic thermostats to kinetic barrier-crossing problems. Last of all, we summarise the lessons learned in this study of three different sorts of applications of our ergodic time-reversible thermostats.

2. Lyapunov exponents – thermostatted harmonic oscillators

The most convincing evidence for the lack of ergodicity with one thermostat variable, and its lack or presence in two-thermostat systems, is the Lyapunov spectrum. Here we concentrate on thermostatted oscillators, the prototypical 'difficult' case. A harmonic oscillator system of four ordinary differential equations, such as the HH, JB, MKT, and PB sets for $(\dot{q}, \dot{p}, \dot{\zeta}, \dot{\xi})$ has four such exponents (λ_1, λ_2, λ_3, λ_4). These exponents describe the deformation of an infinitesimal hypersphere or hypercube in the four-dimensional phase space which contains the motion. Shimada and Nakashima [11], as well as Benettin's group [12] described general approaches to determining the spectrum of exponents.

In an n-dimensional space their algorithms require the solution of $n + 1$ sets of n equations. In addition to a 'reference trajectory' the equations describe the motion of an associated orthonormal set of n comoving basis vectors, centred on the reference trajectory and locating n nearby 'satellite trajectories' in the n-dimensional space. The first Lyapunov exponent gives the time-averaged rate at which two neighbouring solutions of the equations diverge from one another, $\langle\ \dot{\delta}(t) \simeq e^{\lambda_1 t}\ \rangle$. The rate at which the *area* defined by three nearby solutions (the reference and two others) diverges (or converges) $\simeq e^{\lambda_1 t} e^{\lambda_2 t}$ defines λ_2, while the rate at which the volume defined by four solutions and the hypervolume defined by all five of them define λ_3 and λ_4. Although these exponents are typically 'paired' for Hamiltonian systems, with

$$[\lambda_1 \equiv \langle\lambda_1(t)\rangle = -\langle\lambda_4(t)\rangle;\ \lambda_2 \equiv \langle\lambda_2(t)\rangle = -\langle\lambda_3(t)\rangle = 0] \rightarrow \sum_1^4 \lambda_i \equiv 0, \tag{9}$$

with the sum total equal to zero, as implied by Liouville's theorem, none of the two-thermostat systems is Hamiltonian so that this instantaneous symmetry is missing in the time-dependent exponents $\{\lambda(t)\}$. But because the equations of motion are time-reversible, the time-averaged spectra $\langle\lambda(t)\rangle$ *are* symmetric.

Table 1. Long-time-averaged Lyapunov spectrum for the three different thermostats.

Thermostat	λ_1	λ_2	λ_3	λ_4
HH	$+0.068_0$	$+0.000_0$	-0.000_0	-0.068_0
JB	$+0.079_7$	$+0.000_0$	-0.000_0	-0.079_7
MKT	$+0.066_5$	$+0.000_0$	-0.000_0	-0.066_5

For an *ergodic* system the long-time-averaged spectrum of exponents should be *independent* of the initial conditions. In practice, for the harmonic oscillator system, a few hundred oscillations are enough to indicate whether or not a chosen initial condition (either from a grid or chosen randomly) converges to a spectrum close to the unique long-time-averaged Lyapunov spectrum. Estimates of these long-time-averaged exponents, after a *time* $t = 40,000,000$ using a fourth-order Runge–Kutta integrator with an adaptive timestep [20], are shown in Table 1.

The increase in the largest Lyapunov exponent (see λ_1 column of Table 1) with the number of quartic forces (none for MKT, one for HH, and two for JB) suggests, as emphasised by Bulgac and Kusnezov [9], that these terms are particularly well-suited to promote chaos and/or ergodicity. It seems likely that sextic forces, controlling $\langle p^6 \rangle$, would have no particular advantages and would slow numerical work.

The probability densities for the three cases follow easily from the phase-space continuity equation. This makes it easy to check for ergodicity by comparing relatively short-time estimates for the Lyapunov spectrum starting out with initial conditions chosen according to the stationary multivariable Gaussian distributions.

The ergodicity of the MKT oscillator was called into question by Patra and Bhattacharya in 2014 [14], based on apparent 'holes' in a $(q, p, \zeta, \xi) = (q, p, -1, +1)$ double cross-section plane, the analogue of a Poincaré plane for a three-dimensional flow problem. To resolve this question, the subject of the 2014 Ian Snook Prize [15], we chose one million different initial conditions from the appropriate four-dimensional Gaussian distributions for the HH, JB, and MKT cases and determined that *all of them* were fully consistent with a unique chaotic spectrum. Each of these initial conditions was followed for one million fourth-order Runge–Kutta timesteps of 0.005 each.

The alternative possibility, a regular (nonchaotic) solution with all four of the long-time-averaged Lyapunov exponents equal to zero, is easy to distinguish from the chaotic case. As an additional check the velocity moments generated by these three ergodic thermostat types likewise reproduce Gibbs' values for the second, fourth, and sixth velocity moments with five-figure accuracy:

$$\{\langle p^2\rangle, \langle p^4\rangle, \langle p^6\rangle\} = \{1.00000,\ 3.0000,\ 15.000\}.$$

By contrast, the motion equations for a Nosé–Hoover harmonic oscillator (6) at $T = 1$ with unit relaxation time, are known *not* to be ergodic despite their simple three-dimensional Gaussian solution of the phase-space continuity equation. Choosing initial conditions from this stationary distribution $f_{\rm NH} \propto e^{-(1/2)(q^2+p^2+\zeta^2)}$ and measuring the tendency of a nearby initial condition to separate gives the largest *Lyapunov exponent* for the chosen initial condition, $\lambda_1 = \langle (d/dt)(\ln(\delta r)) \rangle$. Because this system is conservative and time-reversible the long-time-averaged Lyapunov spectrum is symmetric, $\{+\ \lambda_1,\ 0,\ -\lambda_1\}$, and sums to zero. 10, 000 initial conditions followed for a time $t = 50,\ 000$ divide neatly into two groups:

$$0.00002 < \lambda_1 < 0.00014\ ;\ 0.006 < \lambda_1 < 0.017.$$

557 initial conditions correspond to a Lyapunov exponent significantly different from zero while 9443 correspond to nonchaotic toroidal solutions for which all three Lyapunov exponents vanish. Evidently roughly 6% of the stationary measure is chaotic (with a positive time-averaged largest Lyapunov exponent). The remaining 94% consists of regular tori with a vanishing Lyapunov spectrum:

$$\langle \lambda_1, \lambda_2, \lambda_3 \rangle = \{0, 0, 0\}.$$

In the language of control theory the Nosé–Hoover equations control the time-averaged value of the kinetic temperature, $\langle (p^2/mk) \rangle \equiv T$. Subsequent work strongly suggests that an ergodic oscillator requires control of at least two moments, not just one. Such an approach requires four or more ordinary differential equations. Bulgac and Kusnezov [9] as well as Ju and Bulgac [10] added a fifth equation so as to be able to thermostat a free particle (or a rotating and translating cluster of particles) undergoing Brownian motion.

The *four*-dimensional phase-space continuity equation shows that both the MKT and the HH thermostats are consistent with exactly the same four-dimensional Gaussian, $f_{\rm HH} = f_{\rm MKT}$. Unlike the Nosé–Hoover single-thermostat model we believe that the three two-thermostat models (HH, JB, and MKT) are *all* ergodic. We believe that this proposition has been thoroughly confirmed by the present work, confirming the chaos of one million independent initial conditions in each case. In view of the lack of other suitable entries in the 2014 competition, we have awarded ourselves the Snook Prize for this finding. It should be noted that *all* of these thermostat models, ergodic or not, *are* time-reversible, with the friction coefficients (ζ, ξ) and the momentum p simply changing sign if the time-ordered sequence of coordinate values $\{q(t)\}$ is reversed. For this reason the time-averaged Lyapunov spectrum is symmetric, with $\lambda_1 + \lambda_4 = \lambda_2 + \lambda_3 = \lambda_2 = \lambda_3 = 0$. Despite the simple analytic nature of the phase-space distribution, the chaos implied by a positive λ_1 engenders an amazing complexity, singular in its spatial behaviour, to which we turn next.

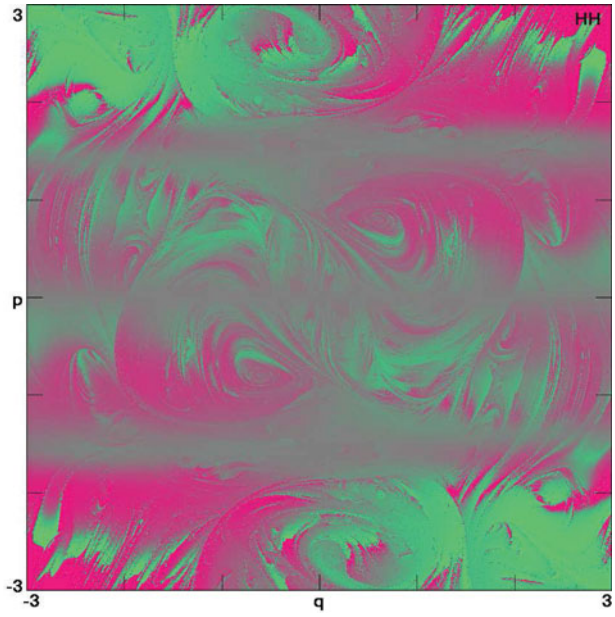

Figure 1. The value of the local (time-dependent) largest Lyapunov exponent for the Hoover–Holian oscillator is shown in the $(q, p, 0, 0)$ plane. Because a mirror reflection of the dynamics (perpendicular to the q axis) changes the signs of both q and p, the figure reveals an inversion symmetry. Red indicates a positive exponent and green a negative. The probability density in the cross-sectional plane is a simple Gaussian in q and p. Nevertheless the local Lyapunov exponents vary in a multifractal manner throughout the four-dimensional space, reflecting their sensitivity to bifurcations in their past histories.

In exploring the HH, JB, and MKT ergodic oscillator solutions we uncovered an amazingly intricate multifractal structure most simply described in terms of the local largest Lyapunov exponent, $\lambda_1(t)$. The three phase-space distributions $\{f(q, p, \zeta, \xi)\}$ are all multidimensional Gaussians of the form

$$f(q, p, \zeta, \xi) \propto e^{-q^2/2} e^{-p^2/2} e^{-\zeta^2/2} e^{-\xi^n/n}, \qquad (10)$$

where n is 2 for HH and MKT and 4 for JB. A closer look, using Lyapunov instability as a tool, reveals the interesting structures shown for the three thermostatted oscillators in Figures 1–3. For completeness, the corresponding Patra–Bhattacharya (PB) cross section is shown in Figure 4.

For each of the three ergodic models we show the value of the local Lyapunov exponent, $\lambda_1(t)$ at the location $(q, p, 0, 0)$ using a continuum of colours with red being the most positive and green the most negative. The plots are analogous to a Poincaré section for the more usual three-dimensional flows. At the equilibrium, $T = 1$, these instability plots can be generated in either of two ways: (1) whenever a $(q, p, 0, 0)$ trajectory comes close to $(\zeta, \xi) = (0, 0)$ plot the value of the corresponding Lyapunov exponent at the location

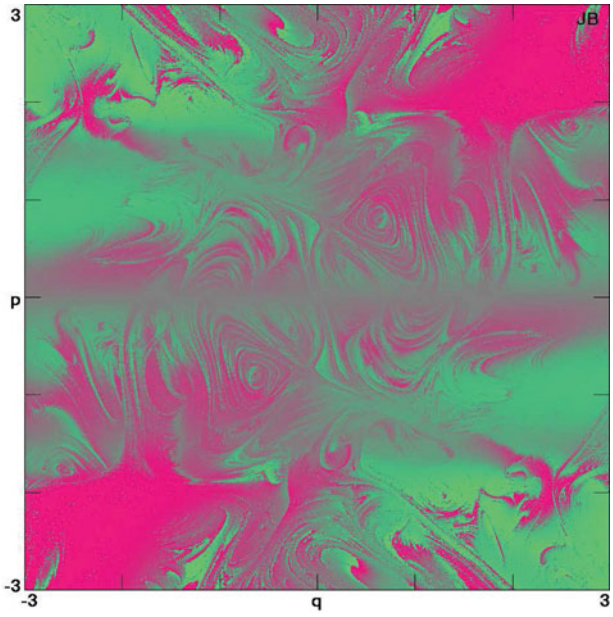

Figure 2. Red indicates a positive local Lyapunov exponent for the ergodic Ju–Bulgac oscillator model. The inversion symmetry is obeyed by all these time-reversible oscillator models. The probability density in the four-dimensional space is Gaussian in q, p, ζ, and ξ^2 as it is also in the $(q, p, 0, 0)$ plane displayed here.

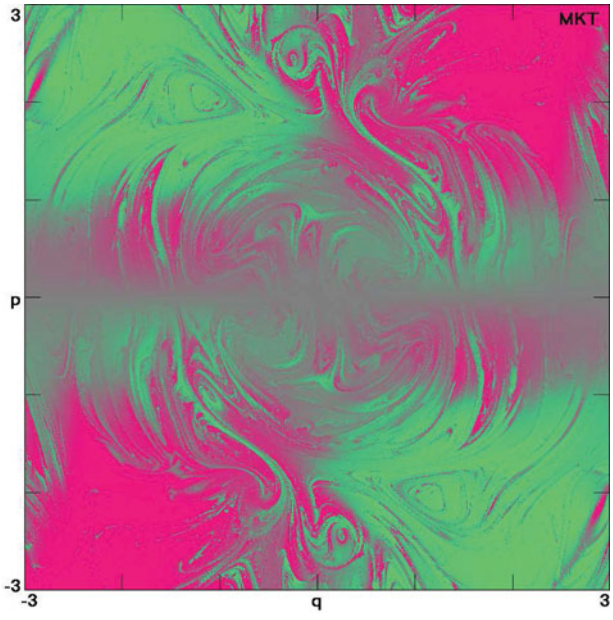

Figure 3. Red indicates a positive Lyapunov exponent and green indicates a negative Lyapunov exponent. If the equations of motion are run backward (by changing the right-hand sides of all four equations) the effect is to reflect the section shown here, changing the sign of q. Like the other models this Martyna–Klein–Tuckerman oscillator has a four-dimensional Gaussian distribution in its (q, p, ζ, ξ) phase space which the dynamics samples ergodically.

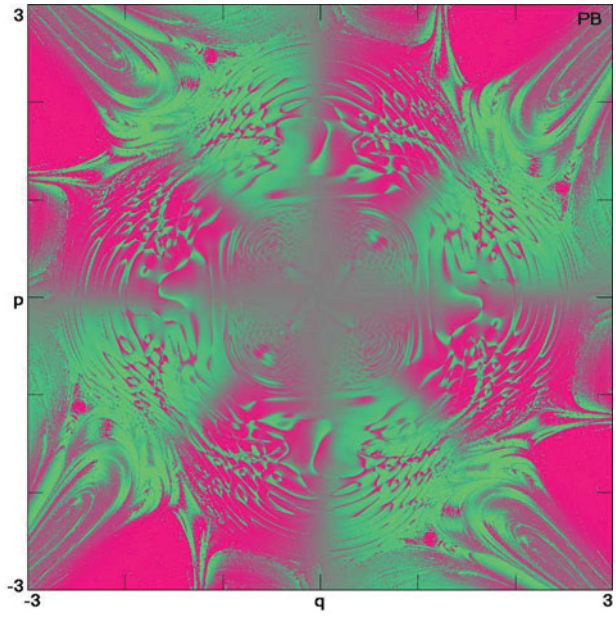

Figure 4. Red indicates a positive Lyapunov exponent and green indicates a negative Lyapunov exponent. If the equations of motion are run backward by changing the right-hand sides of all four equations the effect is to reflect the section shown here, changing the sign of q. Unlike the other two-variable models this Patra–Bhattacharya oscillator does not sample the phase-space ergodically despite having a four-dimensional Gaussian distribution in its (q, p, ζ, ξ) phase space with only about half its measure being chaotic.

(q, p); (2) starting at $(q, p, 0, 0)$ integrate *backwards* in time for several hundred thousand timesteps, storing the backward trajectory. Then process the reversed trajectory data in the forward direction, with Lyapunov instability controlling a nearby constrained satellite trajectory, finding the local Lyapunov exponent at the chosen endpoint location $(q, p, 0, 0)$. It turns out that these two methods are roughly comparable in cost. The second method has the advantage of providing more detail in regions where the measure is small. The precision shown in Figures 1–4 can be generated in simulations taking a day or two on a single processor. Method (2) above, reversing a stored trajectory, is particularly well suited to parallel simulations.

3. Fractals lurk in the simple Gaussian distributions

These cross sections have a fractal look. In fact they are. The reason for this was pointed out in our paper with Dennis Isbister [13]. As the 'past' history of a point is being generated, backward from the 'present', 'bifurcations', where the direction of the trajectory is uncertain at the level of the numerical work limit the trustworthy scale of the Lyapunov exponent when the stored integration is reversed, going forward in time. For the megapixel details shown in Figures 1–4 a few hundred thousand fourth-order (or fifth-order or adaptive) Runge–Kutta timesteps suffice for reliable results

at the resolution of the plotted sections. More detail can always be generated, at a cost exponential in the number of significant figures, by reducing the numerical error of the trajectory integration.

The cross sections shown in the figures have inversion symmetry. As the source of this symmetry is not so obvious let us describe it. Consider a solution of the equations of motion going forward in time, $\{q(t), p(t), \zeta(t), \xi(t), \lambda_1(t)\}$. Viewed simultaneously in a mirror perpendicular to the q axis an observer sees $\{-q(t), -p(t), \zeta(t), \xi(t), \lambda_1(t)\}$. Evidently there is an inversion symmetry, with exactly the *same* Lyapunov exponent at two different values of (q, p):

$$\lambda_1(+q, +p) \equiv \lambda_1(-q, -p).$$

This observation saves a factor of two in computer time. The two-dimensional cross sections where both of the friction coefficients vanish, $\zeta = \xi = 0$ are the starting points for the backward integrations. The figures indicate the magnitude of the largest Lyapunov exponent obtained at the original starting point from a reversed trajectory, with red positive and green negative as the local exponents vary with position. This is the case for positive p.

As is usual, the fluctuations in $\lambda_1(t)$ are an order of magnitude larger than its long-time-averaged value. The variation of the local Lyapunov exponent is not quite continuous. If the local exponent is plotted along a line in the (q, p) plane there are occasional jumps, present on all scales, in the exponent value. The fractal dimension accounts for the variation of the jump magnitudes as a function of resolution. In the MKT case [13] the data along such a line gave a fractal dimension of 1.69 rather than 1.00. Studies of the jumps along such lines reveal their fractal structure, seen here for the first time in two dimensions.

4. Thermostatting configurational temperature?

All three of the two-thermostat HH, JB, and MKT models for heat-bath control of a harmonic oscillator are ergodic. Because of this it was a complete surprise that Patra and Bhattacharya's control (see Equation (8)) of both the kinetic and the configurational [21] oscillator temperatures, using two thermostat variables, was unsuccessful, leading to a mix of regular and chaotic solutions. The stationary phase-space distribution function for the PB equations is the same as that characterising the HH and MKT models (see Equation (10)). But unlike the HH and MKT equations the PB model *fails* the Lyapunov-exponent test for ergodicity. About half the initial conditions chosen from the four-dimensional Gaussian distribution give regular rather than chaotic solutions.

Although controlling *coordinate* moments like $\langle q^2, q^4, q^6 \ldots \rangle$ may seem unphysical Landau and Lifshitz showed (in the 1951 Russian edition of their *Statistical Physics*) that what later came to be termed a 'configurational temperature' [21], based on a mean-squared force, can be derived from Gibbs' canonical distribution. In the canonical ensemble, the mean-squared force is related to the curvature of the potential through the temperature T:

$$kT \int [\nabla^2 \mathcal{H}] e^{-\mathcal{H}/kT} dq \equiv \int [(\nabla \mathcal{H})^2] e^{-\mathcal{H}/kT} dq. \quad (11)$$

So control of $\langle q^2 \rangle$ can be viewed as regulating the fluctuations in the *forces*. This concept is more appealing than coordinate control. But the lack of a physical 'thermometer' capable of measuring force-based temperature is a disabling disadvantage of configurational temperature. The possibility of divergent or negative values of the instantaneous configurational temperature is a further caution flag. The Campisi 'thermostat' is an example of both defects:

$$\mathcal{H} = (p^2/2) + (T/2)\ln(q^2) \rightarrow \{\dot{q} = p;\ \dot{p} = -(T/q)\}. \quad (12)$$

Formally, Campisi dynamics is consistent with a Gaussian momentum distribution. Although at first glance appealing, this simple model exhibits a *negative* configurational temperature, $-T$, in one dimension and a divergent one in two [22]. Disagreement between the kinetic and configurational temperatures is a clear violation of the zeroth law of thermodynamics, to which we turn next.

5. Coupled thermostats – the zeroth law of thermodynamics

To what extent do these minimalistic thermostats, described by one or two additional control variables, exhibit the characteristic properties of macroscopic thermal baths? An essential characteristic of such baths is their consistency with the zeroth law of thermodynamics. Two 'good' thermal baths, both at a temperature T, should, when coupled together or to another canonical equilibrium system at the same temperature T, remain at that common temperature without modifying Gibbs' equilibrium distribution in either bath or in another equilibrium system.

For our thermostatted oscillators this desirable property can be tested by coupling *pairs* of heat baths together with a simple Hooke's-law spring. The modification of the equations of motion for oscillator number 1 and oscillator number 2, both at unit temperature, is as follows:

$$\phi_{12} = (q_1 - q_2)^2/2 \rightarrow \dot{p}_1 = \dot{p}_1(T = 1) + q_2 - q_1;$$
$$\dot{p}_2 = \dot{p}_2(T = 1) + q_1 - q_2, \quad (13)$$

where ϕ_{12} represents the Hookean coupling potential.

It is easy to verify that the two Nosé–Hoover oscillators, coupled together by a spring, have nonergodic solutions, corresponding to a six-dimensional analogue of the

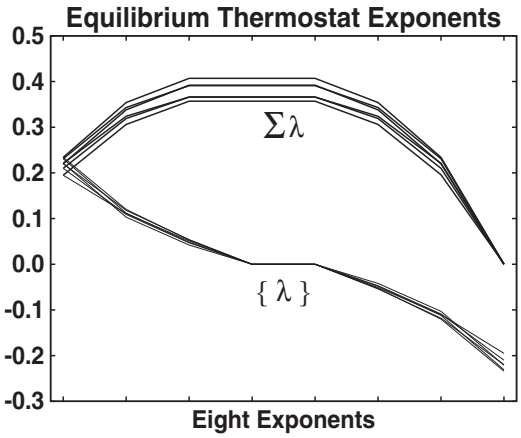

Figure 5. The eight equilibrium Lyapunov exponents describing pairs of ergodic thermostats linked by a Hooke's-law spring exhibit pairing when time-averaged. The JB thermostats exhibit slightly larger Lyapunov exponents due to the quartic terms in their equations of motion. The summed spectra shown in the six upper lines give the growth rates of 1-, 2-, 3-, . . . , 8-dimensional phase volumes. The last sum is precisely zero as the equilibrium equations of motion conserve phase volume when time-averaged.

tori making up most of the single-oscillator phase space. One such solution occurs with initial values of the two oscillator momenta $(p_1, p_2) = (0.99, 1.01)$. Accordingly we restrict our detailed investigation to the three ergodic two-thermostat heat baths to see whether or not they can obey the zeroth law.

All the six combinations of like and unlike *pairs* of ergodic two-thermostat oscillators

$$[\mathrm{HH}+\mathrm{HH},\quad \mathrm{HH}+\mathrm{JB},\quad \mathrm{HH}+\mathrm{MKT},\quad \mathrm{JB}+\mathrm{JB},\quad \mathrm{JB}+\mathrm{MKT},\quad \mathrm{MKT{+}MKT}]$$

provide chaotic eight-dimensional regions in phase space with symmetric Lyapunov spectra. This symmetry implies ergodicity. Figure 5 shows both the spectra and the spectral sums (which give the growth rates of phase-space hyperspheres as functions of their dimensionality). Even though there are relatively small but significant differences between the HH, JB, and MKT Lyapunov exponents, pairing *any two* of these systems together (with a Hooke's-law spring) gives no indication of the dissipation which would result if one phase-space bath were to grow at the expense of the other. We conclude from these six examples that the HH, JB, and MKT heat baths *all* obey the zeroth law of thermodynamics, quite a good outcome for dynamical systems which represent a thermodynamic heat bath with the low cost of only four phase-space dimensions.

The largest Lyapunov exponent in these eight-dimensional problems varies from 0.20 for two coupled MKT oscillators to 0.23 for two coupled JB oscillators. The exponent for two HH oscillators lies in between. Evidently the quartic forces in the JB and HH thermostats are slightly more effective in promoting chaos than are the cubic MKT forces. This same conclusion follows from the time required to generate the structures seen in Figures 1–4. The additional chaos comes at the (rather small) price of an increased stiffness in the differential equations. If any of the three ergodic thermostats were not ergodic we would expect to see a dissipative strange attractor result in coupling it to an ergodic heat bath. In all six pairings of the equilibrium ergodic thermostats there is no evidence of dissipation or reduced phase-space dimensionality. Evidently these three (ζ, ξ) thermostats are good heat baths from the standpoint of the zeroth law of thermodynamics. Coupling pairs of thermostatted oscillators with a harmonic coupling reveals that these three thermostats remain ergodic when coupled and also provides the complete canonical distribution.

6. Nonequilibrium simulations

The similar equilibrium behaviour of the HH, JB, and MKT thermostats suggests a further comparison for simple heat-flow problems in which two coupled thermostats have *different* temperatures, leading to hot-to-cold heat flow and dissipation. Dissipation is reflected in phase space by the formation of strange attractors with a fractional dimensionality reduced below the equilibrium value. In the linear-response regime the six two-bath possibilities must necessarily agree with Green and Kubo's theory as all the two-constant heat baths reproduce Gibbs' canonical (q, p) distribution at equilibrium. Let us be adventurous and treat instead the relatively far-from-equilibrium coupling of two thermostats with thermostat 1 at half the temperature of thermostat 2:

$$\dot{p}_1 = \dot{p}_1(T=1) + q_2 - q_1;\ \dot{p}_2 = \dot{p}_2(T=2) + q_1 - q_2. \tag{14}$$

Just as before all the masses, force constants, and relaxation times are chosen equal to unity.

The far-from-equilibrium Lyapunov data corresponding to the nine combinations of thermostats, with temperatures of 1 and 2, are shown in Figure 6, both individually and as sums. The broad maximum corresponding to sums of three or four exponents indicates that the maximum growth rate in phase space applies to four-dimensional volumes. The summed-up spectrum crosses zero near an abscissa value of 7 indicating that the dimensionality loss for this far-from-equilibrium problem is on the order of 1. Considerably larger losses, comparable to the number of particles, occur in 'ϕ^4-model' chain simulations where each of a few dozen particles is tethered to its lattice site with a cubic restoring force [7].

Closer to equilibrium, with cold and hot temperature of 1.0 and 1.1, all nine thermostat combinations have a Lyapunov sum of order -0.01 while temperatures of 1.0 and 2.0

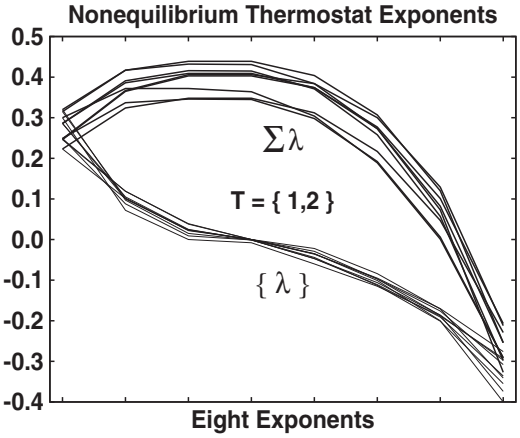

Figure 6. The eight exponents describing the coupling of ergodic thermostats with markedly different temperatures, 1 and 2. Spectra for all nine combinations of thermostats are shown. The hot-to-cold heat current dissipates phase volume. On the average the phase volume approaches zero (a strange attractor) as $\exp[\sum\lambda t] \simeq e^{-0.25t}$ despite the time-reversible nature of all the equations of motion.

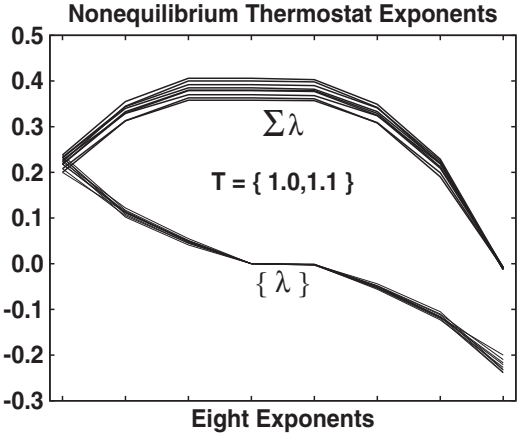

Figure 7. The eight exponents describing the coupling of ergodic thermostats with similar temperatures, 1 and 1.1. All nine combinations are shown. The hot-to-cold heat current could be estimated with linear response theory and is essentially the same for all three thermostat types because the equilibrium phase-space distribution is the same Gaussian for all three thermostat types, $f(q, p) \propto e^{-q^2/2}e^{-p^2/2}$.

provide dissipative sums in the range from -0.20 to -0.30. Compare Figures 6 and 7. Just as in heat conduction according to Fourier's law, we would expect a linear-response dissipation *quadratic* in the temperature difference driving the flow, varying as $(T_{\rm hot} - T_{\rm cold})^2$.

Loss of phase-space volume corresponds to thermodynamic dissipation (through Gibbs' relationship of phase volume to entropy, $S = k\ln\Omega$, where Ω is phase-space volume or the number of states). Coupling two baths, with the cooler bath first, gives the 'entropy production rates ($\dot{S}$)' shown in Table 2. We used quote marks above to remind the reader that simply summing the spectrum is not the same as averaging the dissipation for the cold and hot thermostats.

Table 2. Time-averaged entropy production rate ($\dot{S}$) and Kaplan–Yorke dimension (KYD) for the nine paired thermostats. $\dot{S}$ is the negative sum of the Lyapunov exponents. The first thermostat is kept at $T = 1$ while the second thermostat is kept at $T = 2$.

Paired thermostats	$\dot{S}$	KYD
HH + HH	0.322	7.19
HH + JB	0.254	7.32
HH + MKT	0.213	7.38
JB + HH	0.299	7.16
JB + JB	0.253	7.25
JB + MKT	0.207	7.33
MKT + HH	0.291	7.02
MKT + JB	0.290	7.01
MKT + MKT	0.229	7.17

Dissipation can also be reckoned in terms of the phase-space dimensionality of the dissipative strange attractor, using the Kaplan–Yorke linear interpolation between the last positive dimension and the first negative one. For the nine heat-bath pairings the dimensionalities are shown in Table 2. These results should provide good benchmarks for nonlinear theories of transport.

7. Jumps – equilibrium Mexican hat potential simulations

The double-well 'Mexican hat' potential [8],

$$\phi(q) = -\left[\frac{q^2}{2}\right] + \left[\frac{q^4}{4}\right] \longrightarrow$$
$$\phi(\pm 1) = -\left[\frac{1}{4}\right]\ ;\ \phi(0) = 0, \qquad (15)$$

has a barrier between its two minima of height (1/4). At a temperature of unity, where the barrier is negligible, simulations of the Hat potential coupled to the HH, MKT, and JB thermostats result in excellent agreement with Gibbs' canonical distribution. At sufficiently low temperatures we expect that the frequency of successful jumps over the barrier will decline, as would also be the case using the Metropolis, Rosenbluths, and Tellers' Monte Carlo scheme with a reasonable jump length, perhaps of order 0.01.

A straightforward 'weak coupling' of the two-minimum hat potential to any one of the ergodic oscillator heat baths,

$$\Phi(q_{\rm Bath}, q_{\rm Hat}) = \frac{1}{20}(q_{\rm Bath} - q_{\rm Hat})^2,$$

leads to 'jump' frequencies that vary roughly as Gibbs' canonical barrier weight, $e^{-1/4T}$. Eyring's model, as mentioned in the Wikipedia article on 'Henry Eyring (chemist)',

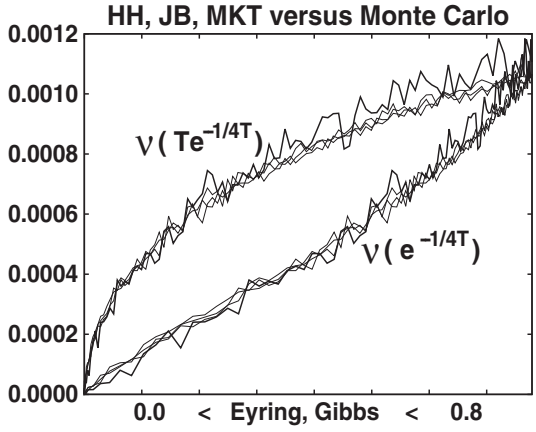

Figure 8. Coupling a Mexican hat potential with twin well depths of 0.25 at $q = \pm 1$ to any of the three ergodic heat baths provides a mechanism for jumping over the barrier. The simulations shown here indicate that all three baths provide essentially the same temperature-dependent jump frequency ν. The dependence is nearly linear when the coupling is small ($\kappa = 1/10$) and the abscissa is Gibbs': $e^{-1/4T}$. Eyring's description (the upper three curves) is shown where the abscissa is now $Te^{-1/4T}$. Gibbs' better approximates an Arrhenius straight line. Monte Carlo simulation of Mexican hat dynamics, with a maximum jump length of $0.009\sqrt{T}$, results in the heavier line plotted in addition to the results for the three heat-bath models.

and with a jump frequency varying as $Te^{-1/4T}$, is a relatively poor description and corresponds to the upper curves in Figure 8. All three ergodic thermostat models behave similarly, as is shown in triplets of narrower lines in Figure 8.

Another possibility for modelling jumps is to use the Metropolis, Rosenbluths, and Tellers' Monte Carlo method. By adjusting the Monte Carlo trial steplength the two approaches, dynamical and Monte Carlo, can be made to correspond. We have compared the number of jumps over the barrier in billion-jump simulations with maximum jump length $dq = 0.009\sqrt{T}$ to dynamical simulations with timestep 0.005, where in all these latter dynamical cases the hat potential is coupled to an HH, MKT, or JB thermostat with temperatures varying from 0.010 to 1.00, as shown in Figure 8.

8. Summary

The Lyapunov spectra for three varieties of time-reversible deterministic oscillator thermostats show that all three of them reproduce an extended (four-variable) form of Gibbs' canonical (two-variable) distribution,

$$f(q, p) = e^{-q^2/2} e^{-p^2/2}/(2\pi).$$

The HH and MKT equations have Gaussian distributions for ζ and ξ while the JB distribution is Gaussian in ζ^2 and ξ. All three approaches are sufficiently robust to thermostat a harmonic oscillator. The three are also consistent with the zeroth law of thermodynamics in the sense that any pair of them at a common temperature T generates Gibbs' canonical distribution for that temperature for both thermostats. With deterministic chaos one has a reproducible replacement for the stochastic approach to thermal mechanics.

This set of ergodic thermostats represents a good toolkit for simulations with a few degrees of freedom as it gives an idea of the dependence of dissipation on the chosen form of the thermostat. With many degrees of freedom, where ergodicity is not an issue (Poincaré recurrence takes forever so that the size of fluctuations determines the usefulness of the results) any of these thermostats, as well as the single thermostat Nosé–Hoover model, is likely equally useful.

We have considered two *nonergodic* time-reversible thermostats, the PB and Nosé–Hoover, which reproduce the specified kinetic temperature but do not reproduce all of Gibbs' canonical distribution. When the PB or NH thermostats are coupled to the HH, JB, or MKT thermostats two qualitatively different results occur: (1) a dissipative strange attractor in the case of the PB model and (2) a conservative integer-dimensional chaotic sea when coupled to the Hamiltonian-based Nosé–Hoover oscillator. These results are similar for each of the three ergodic thermostats. In the PB case the dissipation is an indicator of the non-Hamiltonian nature of the dynamics. Any of the ergodic thermostats, HH, JB, or MKT, can be used successfully in both equilibrium and nonequilibrium simulations.

The first two of these can also be applied in nonequilibrium simulations where it is desired to specify the kinetic temperature of selected degrees of freedom. Though there is no problem in solving the MKT equations for nonequilibrium problems Brad Holian pointed out long ago [18] that this thermostat fails to return its target temperature due to the nonzero correlation linking the two MKT friction coefficients, $\langle \zeta\xi \rangle^{\rm noneq}_{\rm MKT} \neq 0$.

This relatively thorough investigation of ergodicity, based on one million independent initial conditions, should settle (at least from the numerical, as opposed to analytical, viewpoint) the question of the ergodicity of the MKT oscillator. The apparent 'holes' in that oscillator's cross section are still a small 'puzzle'. A second such 'puzzle' is the nature of the local Lyapunov exponents. Their intricate multifractal Lyapunov structure is well concealed within an innocent Gaussian distribution.

From the standpoint of dynamical systems theory (as opposed to thermodynamics) we wish to emphasise the amazing nature of the chaos hidden within the simple ergodic Gaussian distributions. The smoothness of the distributions and the good convergence of their moments conceal the fractal nature of their chaos, as shown in Figures 1–3. We recommend all three systems for further studies. The ($\zeta = \xi = 0$) plane is only a single choice among the many possible. Despite their fractal nature the cross-sectional values are well-behaved, accessible, and reproducible from the numerical standpoint. It is encouraging for the future that

work originally chosen to settle some ergodicity questions turned out to generate a swarm of other problems still needing more detailed understanding.

Acknowledgements

We thank Aurel Bulgac and Baidurya Bhattacharya for their able help.

Disclosure statement

No potential conflict of interest was reported by the authors.

References

[1] W.G. Hoover and B.J. Alder, J. Chem. Phys. **46**, 685 (1967).
[2] S. Nosé, J. Chem. Phys. **81**, 511 (1984).
[3] S. Nosé, Mol. Phys. **52**, 191 (1984).
[4] W.G. Hoover, Phys. Rev. A **31**, 1695 (1985).
[5] H.A. Posch, W.G. Hoover, and F.J. Vesely, Phys. Rev. A **33**, 4253 (1986).
[6] W.G. Hoover and C.G. Hoover, *Time Reversibility, Computer Simulation, Algorithms, Chaos* (World Scientific, Singapore, 2012).
[7] W.G. Hoover and C.G. Hoover, *Simulation and Control of Chaotic Nonequilibrium Systems* (World Scientific, Singapore, 2015).
[8] D. Kusnezov, A. Bulgac, and W. Bauer, Ann. Phys. **204**, 155 (1990).
[9] A. Bulgac and D. Kusnezov, Phys. Rev. A **42**, 5045 (1990).
[10] N. Ju and A. Bulgac, Phys. Rev. B **48**, 2721 (1993).
[11] I. Shimada and T. Nagashima, Prog. Theor. Phys. **61**, 1605 (1979).
[12] G. Benettin, L. Galgani, A. Giorgilli, and J. M. Strelcyn, Meccanica **15**, 9 (1980).
[13] W.G. Hoover, C.G. Hoover, and D.J. Isbister, Phys. Rev. E **63**, 026209 (2001).
[14] P.K. Patra and B. Bhattacharya, Phys. Rev. E **90**, 043304 (2014). arχiv : 1407.2353.
[15] W.G. Hoover and C.G. Hoover, Comput. Methods Sci. Technol. **20**, 87 (2014).
[16] P.K. Patra and B. Bhattacharya, arχiv: 1411.2194 (2014).
[17] G.J. Martyna, M.L. Klein, and M. Tuckerman, J. Chem. Phys. **97**, 2635 (1992).
[18] W.G. Hoover and B.L. Holian, Phys. Lett. A **211**, 253 (1996).
[19] P.K. Patra and B. Bhattacharya, J. Chem. Phys. **140**, 064106 (2014).
[20] W.H. Press, B.P. Flannery, S.A. Teukolsky, and W.T. Vetterling, *Numerical Recipes: The Art of Scientific Computing*, 3rd ed. (Cambridge University Press, Cambridge, 2007).
[21] C. Braga and K.P. Travis, J. Chem. Phys. **123**, 134101 (2005).
[22] D. Sponseller and E. Blaisten-Barojas, Phys. Rev. E **89**, 021301(R) (2014).